FARADAY

Classical theories of reaction dynamics: Transition state theory, spatial diffusion controlled reactions, and the energy diffusion limit†

Bruce J. Berne[a] **and Michal Borkovec**[b]

[a] *Department of Chemistry and Center for Biomolecular Simulations, Columbia University, New York, NY 10027, USA*
[b] *Department of Chemistry and Center for Advanced Materials Processing, Clarkson University, Potsdam, NY 13699-5814, USA*

Received 3rd March 1998, Accepted 25th March 1998

The calculation of chemical reaction rate constants is of importance to much of chemistry and biology. Here we outline useful theoretical methods and numerical techniques for single and many dimensional systems for weak and strong collision models and discuss connections between different theories from a unified point of view.

I Introduction

A paradigm for activated barrier crossing is motion on a one dimensional bistable double well potential. If the barrier energy is much higher than the thermal energy $k_B T$ most of the molecules will be located near one of the two minima. The reacting molecule suffers collisions with bath molecules which will perturb the motion of the reaction coordinate in a random fashion. Those random perturbations will allow the molecule to cross between the two metastable wells and react. Because a typical barrier is high compared to $k_B T$ the molecule will spend a very long time near a metastable minimum and only extremely rarely cross to the other side. Ensemble averages over such trajectories lead to microscopic chemical rate laws. Since the recrossings are very seldom it is expected that subsequent recrossings will be random and uncorrelated *i.e.* Poissonian. Recent theoretical progress in treating solvent effects on reaction rate theory has been reviewed in several comprehensive reviews.[1,2]

More formal definitions of rate constants have been given.[3] The oldest definitions of the rate constant are based on steady state flux ideas. Also the eigenvalue spectrum of the time evolution operator, correlation functions, as well as mean first passage times are popular ways of defining rate constants. If the rate constant is well defined (*i.e.* if $\beta Q \gg 1$ where Q is the activation energy, $\beta^{-1} = k_B T$, k_B is Boltzmann's constant and T is the absolute temperature) all definitions give the same results. More precisely, the different definitions yield identical rate constants up to exponentially small terms of $O[\exp(-\beta Q)]$ compared with terms of order unity. Unfortunately, there are very few models for which the rate constant is known exactly *i.e.* up to such exponentially small terms. One example is a one dimensional diffusion process. Frequently, however, the analysis of a problem is not tractable to this exponential small order but one can evaluate only the leading contribution to the rate constant and one neglects algebraically small terms of order $[1/(\beta Q)]$ compared to terms of order unity. An example is the famous Kramers expression for the rate constant in the regime of intermediate to high friction.[4]

Even though different approaches yield the same results they vary in usefulness. Correlation functions are very powerful for numerical evaluation of rate constants. The reactive flux correlation function describes the time evolution of the population given the system started at the barrier top. This function will plateau at a value which can be related to the rate constant.[5–9] Generally the plateau value will be reached on a microscopic timescale so that simulations do not have to be run for exponentially long times. Mean first passage times which are in many ways equivalent to steady state flux ideas are useful for analytical studies.[3] There has been substantial progress in applying boundary layer techniques for solving mean first passage time equations. These techniques were mainly introduced in the work by Matkowsky and Schuss.[10] We will rely heavily on such techniques in Section III. Most of the ideas outlined above can be applied to unimolecular isomerization reactions and dissociation reactions as well to bimolecular recombination reactions and atom transfer reactions.

Since the full many-body dynamics of a molecule in a liquid is complicated one often focuses on simple stochastic models. The idea is to replace the bath gas or liquid by a stochastic bath. There are two broad classes of stochastic models. In the first class one defines a particular model that applies to only a relatively narrow pressure range. The unimolecular rate theory of gas phase reactions which describes dissociation reactions at low pressures,[11–13] is such a model. Within this approach master equations in energy space are considered. Another example is the theory of diffusion controlled reactions in dense liquids based on the work of Smoluchowski.[1,14,15] Here one treats the diffusion equations in position space. On the other hand there are more broad based stochastic models that apply over the whole density regime. The original approach of Kramers[4] belongs to this second class. In this case a frictional Langevin equation models the solvent at all densities. In recent years many models applicable over wide density ranges have been proposed. For example general impulsive collisional models which re-sample velocities from a given distribution function at a given collision frequency were discussed by Skinner and Wolynes,[16,17] Montgomery *et. al.*[8] and Berne *et. al.*[18] The popular BGK

---

† This paper was to have been presented at Faraday Discussion 110, University of St. Andrews, 1st–3rd July 1998, but was withdrawn because the author was ill and therefore unable to attend the meeting.

model[19] is a particular impulsive collisional model which resamples velocities from a Maxwell–Boltzmann distribution upon a collision. If a collision changes the velocity only infinitesimally one recovers the Kramers model (see Skinner and Wolynes[17]). Non-Markovian Langevin models have been proposed by Grote and Hynes[20] where the frequency dependence of the friction kernel describes the finite solvent relaxation times. The original Kramers model utilizes a frequency independent friction kernel.

Usually such general models which are applicable over a wide density range reduce to the more classical models of the first group *i.e.* to unimolecular rate theory at low collision frequencies or frictions and to theory of diffusion controlled reactions at high collision rates or frictions. Until now all these theories have been developed quite independently and therefore do not incorporate the various interconnections between these different approaches. By exploiting these interconnections we show that much insight into the problems can be gained.

In all cases given a stochastic model, one is faced with the problem of calculating the rate constant. This is a nontrivial problem. It can be done numerically as well as analytically in some cases. Transition state theory always provides an upper bound for the rate constant. This is briefly considered in Section II. In the low pressure (or infrequent collision, small damping) regime the rate constant is determined by a Master equation in energy space. If the model has a diffusion controlled limit (as for most collisional models at high collision frequencies) one can evaluate the rate constant in the diffusion controlled regime. We present in Section III A a general approach based on asymptotic techniques. Surprisingly it is relatively easy to construct trivial interpolation formulae which give reasonable predictions of the rate constants over the whole friction or collision frequency range. We consider these ideas in Sections IV C and IV D where we also compare some of the analytical results with numerical simulations.

II Transition state theory

A General analysis

The transition state rate constant is most conveniently found from the short time behavior of the reactive flux as described by Pechukas[21,22] and Chandler.[7] This gives for the rate constant from reactants to products

$$k_{\mathrm{TST}} = \frac{\langle \delta(f)\dot{f}\theta(\dot{f})\rangle}{\langle \theta(f)\rangle} \tag{1}$$

where $\theta(.)$ is the Heaviside step function, $\delta(.)$ the Dirac delta function and $\langle \ldots \rangle$ represents a canonical average. The reaction coordinate f is a function of internal coordinates of the molecule which is positive for reactants and negative for products. As an example, the reaction of butane from *trans* to *gauche* states we may define $f = \phi - \phi_{\mathrm{T}}$ where ϕ is the dihedral angle and ϕ_{T} is chosen near the location of the *trans–gauche* saddle. With a reaction coordinate f, the transition state rate constant at a particular temperature can be evaluated for a given potential energy surface and masses of the nuclei. Even though any reaction coordinate f which vanishes near the saddle point is acceptable there is an optimum choice. Since the transition state theory gives an upper bound for the true rate constant[21] the best choice for the reaction coordinate f is that which minimizes the transition state rate constant. Such a choice is in the spirit of variational canonical transition theory.[23] Before we make such an optimal choice let us simplify eqn. (1) by performing the velocity integral explicitly. This yields

$$k_{\mathrm{TST}} = \frac{1}{\sqrt{2\pi\beta}} \frac{\langle \delta(f) | M^{-1/2}\nabla_r f | \rangle}{\langle \theta(f)\rangle} \tag{2}$$

which involves an average over configurational coordinates only. These coordinates are the positions of the nuclei $\boldsymbol{r} = (r_1, r_2, \ldots, r_{3N})$ where N is the number of nuclei in the molecule. We have denoted $\beta = 1/k_{\mathrm{B}}T$ and abbreviated

$$| M^{-1/2}\nabla_r f |^2 = \sum_i \frac{1}{m_i}\left(\frac{\partial f}{\partial r_i}\right)^2 \tag{3}$$

where m_i are the masses of the nuclei in the molecule. This quantity is proportional to a diagonal element in the Wilson G-matrix.[24] Eqn. (2) can be simplified further by integrating over the coordinates describing the center of mass position and the orientation of the molecule. This is possible since the reaction coordinate $f(\boldsymbol{q})$ and the potential energy $U(\boldsymbol{q})$ depend only on the internal coordinates $\boldsymbol{q}$. These internal coordinates can be bond lengths, bond angles *etc.* and are denoted by $q = (q_1, q_2, \ldots, q_m)$ where m is the number of internal degrees of freedom *i.e.* $m = 1$ for a diatomic and $m = 3N - 6$ for a polyatomic molecule. Let us introduce a Jacobian $J(\boldsymbol{q})$ for the transformation from Cartesian coordinates $\boldsymbol{r}$ to internal coordinates $\boldsymbol{q}$. This integrated Jacobian is the determinant of the metric tensor times the integral over the center of mass coordinate giving a factor V, the volume of the system and factors resulting from integrations over the orientational degrees of freedom. Examples of this quantity will be given later.

We introduce the configurational partition function of reactants

$$Z_{\boldsymbol{r}} = \mathrm{d}\boldsymbol{r}\mathrm{e}^{-\beta U(\boldsymbol{q})}\theta[f(\boldsymbol{q})] = \int \mathrm{d}\boldsymbol{q} J(\boldsymbol{q})\mathrm{e}^{-\beta U(\boldsymbol{q})}\theta[f(\boldsymbol{q})] \tag{4}$$

where $U(\boldsymbol{q})$ is the intramolecular potential. This partition function $Z_{\boldsymbol{r}}$ can be evaluated by steepest descent. There are a few points to note. First we have to remember that every equivalent reactant minimum contributes in the same way, *e.g.* there are two equivalent *gauche* states in butane which would give a factor of two in this case. Second, for unbound reactants (*e.g.* recombination) we will obtain a further factor of the volume V of the system. This fact will lead to a rate constant which is inversely proportional to the volume of the system. In biomolecular reaction kinetics it is customary to drop this volume factor and refer to a biomolecular rate constant per unit volume.

At this point we can rewrite eqn. (1) as

$$k_{\mathrm{TST}} = \frac{1}{\sqrt{2\pi\beta}} \frac{1}{Z_{\boldsymbol{r}}} \int \mathrm{d}\boldsymbol{q}\mathrm{e}^{-\beta U(\boldsymbol{q})} J(\boldsymbol{q}) | M^{-1/2}\nabla_{\boldsymbol{r}} f | \delta[f(\boldsymbol{r})] \tag{5}$$

Let us now pick the optimal reaction coordinate f which minimizes the transition state rate constant. First of all $f(\boldsymbol{q})$ has to vanish at the saddle point of the potential energy hypersurface to obtain the most favorable Boltzmann factor. At low temperatures we can expand the potential energy around the saddle up to quadratic terms and therefore only worry about a reaction coordinate linear in the displacements in the internal coordinates. The most favorable orientation of the reaction coordinate can usually be shown to be normal to the only unstable mode of the potential energy surface. In the low temperature limit we can perform the integral by steepest descent which gives

$$k_{\mathrm{TST}} \approx \frac{1}{\sqrt{2\pi\beta}} \frac{1}{Z_{\boldsymbol{r}}} \frac{| M^{-1/2}\nabla_{\boldsymbol{r}} f |_T}{| \nabla_{\boldsymbol{q}} |_T} \mathrm{e}^{-\beta U(\boldsymbol{q}_{\mathrm{T}})} \left(\frac{2\pi}{\beta}\right)^{m-1/2} \times \frac{1}{\sqrt{f_2 f_3, \ldots, f_m}} \tag{6}$$

We use the $\approx$ sign instead of the equality sign to remind ourselves that we have neglected terms of order $(\beta Q)^{-1}$ compared to unity. The subscript T denotes that the quantity in question is evaluated at the saddle point $\boldsymbol{q} = \boldsymbol{q}_{\mathrm{T}}$. We have denoted by $f_2, f_3, \ldots, f_m$ the positive eigenvalues of the force constant matrix

$$F_{ij} = \left(\frac{\partial^2 U_{\mathrm{eff}}}{\partial q_i\, \partial q_j}\right)_T \tag{7}$$

Since the transition state is a saddle point this matrix has one negative eigenvalue f_1 which does not enter the result but will be important later in the discussion of diffusion controlled reactions. We have introduced an effective potential (see also Rodger and Sceats[25])

$$U_{\mathrm{eff}}(\boldsymbol{q}) = U(\boldsymbol{q}) + U_m(\boldsymbol{q}) \tag{8}$$

where

$$U_m(\boldsymbol{q}) = -k_{\mathrm{B}}\, T \ln J(\boldsymbol{q}) \tag{9}$$

is a 'metric potential.' In general the saddle point must be located on the effective potential $U_{\mathrm{eff}}(\boldsymbol{q})$. This potential can be thought of as a potential of mean force arising from centrifugal distortion. This is analogous to the potential of mean force in a liquid which similarly modifies the potential surface of a molecule (see for example Chandler[26]). In the case where the bare potential $U(\boldsymbol{q})$ has a well defined saddle point the variation of the metric potential becomes negligible in the low temperature limit and can simply be replaced by a constant. Under these circumstances the metric potential modifies the rate constant by a multiplicative factor. In the case where there is no saddle point on the bare potential surface (as on a dissociative potential) only the effective potential which includes the metric contribution has a meaningful saddle point and must be used to locate the transition state. Note that in this case of equivalent transition states we have to count each contribution separately *e.g.* we pick up a factor of two calculating the rate from *trans* to *gauche* butane. The case of a pseudorotating transition state as occurs in cyclohexane[27] for example would be indicated by a zero eigenvalue of F. In this case eqn. (6) does not apply since one has to integrate over this mode explicitly.

III Diffusion controlled reactions

A Asymptotic analysis

In the spatial diffusion regime the distribution function of the molecule in position space of all the nuclei $\boldsymbol{r} = (r_1, r_2, \ldots, r_{3N})$, where N is the number of nuclei in the molecule, will be described by a diffusion equation

$$\frac{\partial P(\boldsymbol{r}, t)}{\partial t} = \sum_i \frac{\partial}{\partial r_i} (\bar{\mathrm{A}}_i P) + \sum_{i,\, j} \frac{\partial^2}{\partial r_i \partial r_j} (\bar{D}_{ij} P) \tag{10}$$

$\bar{D}_{ij}$ is the diffusion tensor of the molecule in position space and the drift satisfies detailed balance

$$\bar{A}_i = \frac{1}{\bar{P}_{\mathrm{eq}}} \sum_j \frac{\partial}{\partial r_j} (\bar{D}_{ij} \bar{P}_{\mathrm{eq}}) \tag{11}$$

Here $\bar{P}_{\mathrm{eq}}$ is the equilibrium distribution function and

$$\bar{P}_{\mathrm{eq}}(\boldsymbol{r}) \propto \mathrm{e}^{-\beta U(\boldsymbol{r})} \tag{12}$$

where $U(\boldsymbol{r})$ is the internal potential of the molecule and $\beta = 1/k_{\mathrm{B}}\, T$. Since the potential energy depends on the internal coordinates $\boldsymbol{q} = (q_1, q_2, \ldots, q_m)$ only, *i.e.* $U(\boldsymbol{r})$, we can explicitly integrate eqn. (10) over the center of mass and orientational degrees of freedom to obtain

$$\frac{\partial P(\boldsymbol{r}, t)}{\partial t} = \epsilon \sum_i \frac{\partial}{\partial r_i} (\bar{A}_i P) + \epsilon^2 \sum_{i,\, j} \frac{\partial^2}{\partial r_i \partial r_j} (\bar{D}_{ij} P) = LP \tag{13}$$

where

$$\bar{A}_i = \frac{\epsilon}{\bar{P}_{\mathrm{eq}}} \sum_j \frac{\partial}{\partial r_j} (\bar{D}_{ij}) \tag{14}$$

Eqn. (13) is a diffusion equation of the same form as eqn. (10) but it is written in terms of the internal coordinates $\boldsymbol{q}$ of the molecule. We have introduced a parameter ϵ which will be used later to perform asymptotic expansions. It is essentially the barrier height compared to thermal energy if one introduces properly scaled dimensionless variables. For the sake of simplicity we will use variables carrying proper dimensions and set $\epsilon = 1$ at the end of the calculation. Even though the internal coordinates again satisfy a diffusion equation the equilibrium distribution function as well the diffusion coefficients in eqn. (13) and (14) are modified. The equilibrium distribution becomes

$$P_{\mathrm{eq}}(\boldsymbol{q}) \propto J(\boldsymbol{q}) \mathrm{e}^{-\beta U(\boldsymbol{q})} \tag{15}$$

where $J(\boldsymbol{q})$ is the orientationally averaged Jacobian. The diffusion coefficients in internal coordinates are

$$D_{ij}(\boldsymbol{q}) = \sum_{k,\, l} \frac{\partial q_i}{\partial r_k} \frac{\partial q_j}{\partial r_l} \bar{D}_{kl} \tag{16}$$

since they form a contravariant tensor.

The rate constant is evaluated as the inverse of the mean first passage time. We have to solve (see Gardiner[3])

$$L^{\dagger} T = -1 \tag{17}$$

where

$$L^{\dagger} = \epsilon \sum_i A_i(\boldsymbol{q}) \frac{\partial}{\partial q_i} + \epsilon^2 \sum_{ij} D_{ij}(\boldsymbol{q}) \frac{\partial^2}{\partial q_i\, \partial q_j} \tag{18}$$

$L^{\dagger}$ is the adjoint of the diffusion operator L introduced in eqn. (13). Even though one could solve eqn. (17) with absorbing boundary conditions in the product well, a more practical and equivalent procedure has been used by Matkowski and Schuss.[28,29] One calculates the mean first passage time from the bottom of the well to the separatrix $\partial\Omega$ which encloses the reactant region Ω. The separatrix is a hypersurface in position space from which a trajectory has equal probability to return into the reactant well or to proceed into the product well. One half of the inverse of the mean first passage time to the separatrix is then the rate constant. The location of the separatrix is found by analyzing the stochastic equation of motion corresponding to eqn. (13)

$$\dot{q}_i = A_i(\boldsymbol{q}) + \xi_i \tag{19}$$

where ξ_i is the corresponding white noise source. In the low temperature limit, *i.e.* as $\epsilon \to 0$, we can neglect the noise term and the fate of a trajectory started near the saddle will be determined by the linearized form of eqn. (19).

$$\delta \dot{q}_i = -\beta \sum_{i,\, k} D_{ij} F_{jk} \delta q_k \tag{20}$$

where we have used the force constant matrix F_{ij} evaluated at the saddle [*cf.* eqn. (7)]. The diffusion tensor entering eqn. (20) is evaluated at the saddle point as well. We denoted the deviation from the location of the saddle by $\delta \boldsymbol{q} = \boldsymbol{q} - \boldsymbol{q}_{\mathrm{T}}$. Let us determine the fate of a trajectory which we start close to the saddle point. The eigenvalue equation for the left (note that $\boldsymbol{DF}$ is non-symmetric) eigenvectors

$$\boldsymbol{DF} u_i = \lambda_i u_i \tag{21}$$

governs the behavior of these trajectories. Since $\boldsymbol{D}$ is definitely positive and only one eigenvalue of $\boldsymbol{F}$ is negative there will usually be a single left eigenvector of $\boldsymbol{DF}$ corresponding to an unstable mode ($\lambda_1 < 0$). The eigenvectors corresponding to the stable positive eigenvalues ($\lambda_2, \lambda_3, \ldots, \lambda_m$) will span a hypersurface which is the separatrix. If we start a trajectory lying in the separatrix it will converge to the saddle point; a trajectory not lying in the separatrix will move away from the saddle.

This results in a characteristic structure of the mean first passage time $T(\boldsymbol{q})$. The quantity $T(\boldsymbol{q})$ will change very rapidly along the normal unit vector $\hat{\boldsymbol{n}}$ to the separatrix. The mean first passage time will develop a boundary layer solution which can be analyzed by setting

$$T(\boldsymbol{q}) = Cv(\boldsymbol{q}) \tag{22}$$

It turns out that C is exponentially large so we have to solve only

$$L^{\dagger}v = 0 \tag{23}$$

Transforming to local coordinates at the saddle point and introducing a stretched variable $\eta = z/\sqrt{\epsilon}$ where $z = \hat{\boldsymbol{n}}\cdot(\boldsymbol{q} - \boldsymbol{q}_T)$ we find that as $\epsilon \to 0$ the boundary layer structure is determined by the solution of

$$D_{nn}\frac{\partial^2 v}{\partial \eta^2} + A_{n(1)}\eta\frac{\partial v}{\partial \eta} \approx 0 \tag{24}$$

where

$$D_{nn} = \sum_{i,j} n_i n_j D_{ij}(\boldsymbol{q}_T) \tag{25}$$

and

$$A_n^{(1)} = \left(\frac{\partial A_n}{\partial \eta}\right)_{q=q_T} \tag{26}$$

with

$$A_n = \sum_i n_i A_i(\boldsymbol{q}) \tag{27}$$

Note that the drift A vanishes at the saddle which makes it necessary to keep the lowest non-vanishing term of the Taylor expansion of this quantity near the saddle. The structure of the boundary layer which is the solution of eqn. (24) is a simple error function

$$v(\eta) = \sqrt{\frac{2\gamma}{\pi}}\int_0^{\eta} d\eta'\, e^{-\gamma\eta'^2/2} \tag{28}$$

where we made use of the boundary conditions $v(\eta) = 0$ for $\eta = 0$ and $v(\eta) \to 1$ for $\eta \to \infty$. We have used the abbreviation

$$\gamma = \left|\frac{A_{n(1)}}{D_{nn}}\right| \tag{29}$$

Note that this case is different from the cases discussed in the literature[1] where the drift A does not vanish and leads to an exponential boundary layer of thickness ϵ. Here the drift A vanishes linearly at the separatrix which leads to an error function boundary layer of thickness $\sqrt{\epsilon}$.

Given the boundary layer solution we can evaluate the undetermined constant C. This is done by the standard trick of multiplying eqn. (13) by $P_{\text{eq}}(\boldsymbol{q})$ and integrating over Ω. Using the Gauss divergence theorem we find

$$-C\epsilon^2\int_{\partial\Omega} dSP_{\text{eq}}(\boldsymbol{q}_s)\sum_{ij} n_i D_{ij}\frac{\partial v}{\partial q_j} = \int_{\Omega} d\boldsymbol{q}P_{\text{eq}}(\boldsymbol{q}) \tag{30}$$

Since the particle has equal probability to reach either well from the separatrix the rate constant k is $1/(2C)$. Inserting eqn. (28) into eqn. (30) and performing the integrals by steepest descent we find after some algebra that

$$k \approx \frac{|\lambda_1|}{\sqrt{|f_1|}}\frac{|\nabla_{\boldsymbol{q}} f|}{|M^{-1/2}\nabla_r f|_T}k_{\text{TST}} \tag{31}$$

where λ_1 and f_1 are the negative eigenvalues of $\boldsymbol{DF}$ and $\boldsymbol{F}$, respectively. We used the rate constant k_{TST} given by canonical transition state theory eqn. (6). Since the matrix $\boldsymbol{DF}$ governs the equation of motion near the saddle eqn. (31) looks similar to the Grote–Hynes relation[20] or the equivalent expression obtained by Langer.[30]

B Applications

It is quite easy to see that in the case of no rotations and isotropic mass and diffusion tensor eqn. (31) reduces to the result derived by Landauer and Swanson[31]

$$k = \frac{\omega_B}{\gamma}k_{\text{TST}} \tag{32}$$

where k_{TST} is given by

$$k_{\text{TST}} \approx \frac{1}{2\pi}\frac{\prod_i \omega_i^{(0)}}{\prod_i \omega_i^{(S)}}e^{-\beta Q} \tag{33}$$

γ is the mass weighted friction and ω_{B} is the frequency of the unstable normal mode of the saddle. If the rotational contributions are negligible $[J(\boldsymbol{q}) = 1]$ one can show that eqn. (31) is exactly equivalent to Langer's expression. Eqn. (31) is also equivalent to the diffusion controlled limit (high friction limit) of the Grote–Hynes relation applied to the general case of coupled modes of anisotropic mass and friction. This situation neglects rotational corrections and has been discussed by Grote and Hynes[32] and van der Zwan and Hynes[33] in some detail.

However, if the rotational degrees of freedom contribute there are differences. First, the reactive frequency determined by the interaction plus the metric potential will not in general coincide with the barrier frequency given by the potential surface alone. In the case of a well defined saddle point on the surface $U(\boldsymbol{q})$ the metric potential contribution is negligible. However, on a surface with no saddle point (as in a dissociation reaction) the curvature of this saddle in the effective potential will determine the diffusion controlled fall-off. The simplest example of a nontrivial rotational effect is the recombination of a diatomic. We want to show that eqn. (31) applied to a diatomic molecule reduces correctly to the recombination rate constant evaluated by Smoluchowski in 1917

$$k = 4\pi(D_1 + D_2)a \tag{34}$$

where D_1 and D_2 are the diffusion coefficients of the individual atoms of the diatomic molecule. For a general potential Debye[34] showed that

$$a^{-1} = \int_{r_e}^{\infty} dr\,\frac{e^{-\beta U(r)}}{r^2} \tag{35}$$

and r_e is the location of the minimum as well. It is worthwhile mentioning that in one and two dimensions the diffusion controlled rate constants do not exist. It turns out that the square in the integrand of eqn. (35) is actually the number of spatial dimensions minus one which makes the integral diverge in one or two dimensions. Again this is an anomaly of recombination reactions in less than three dimensions.[35,36] To show the equivalence of eqn. (31) and (34) we expand the integrand in eqn. (35) around its maximum $r = r_T$ to second order and replace the integral by a Gaussian. Note that this was how the location of the transition state was determined in Section II where we used the reaction coordinate $f = r - r_T$. Using

$$k_{\text{TST}} = \sqrt{\frac{8\pi}{\mu\beta}}r_T^2\,e^{-\beta Q} \tag{36}$$

we can collect terms which give us a factor of k_{TST} and obtain

$$k = \beta\sqrt{\mu}(D_1 + D_2)\left[-\left(\frac{\partial^2 U_{\text{eff}}}{\partial r^2}\right)_{r=r_T}\right]^{1/2}k_{\text{TST}} \tag{37}$$

Using the effective potential

$$U_{\mathrm{eff}}(r) = U(r) - 2k_{\mathrm{B}}T \log r \tag{38}$$

we find that eqn. (34) is asymptotically equal to eqn. (37).

Let us apply this relation to the case of a polyatomic of isotropic mass m and isotropic diffusion tensor $\boldsymbol{D}$. Furthermore assume that one of the internal coordinates is the reaction coordinate f. Then we obtain

$$k = \frac{\omega_{\mathrm{B}}}{\gamma} k_{\mathrm{TST}} \tag{39}$$

where the mass weighted friction coefficient is

$$\gamma = \frac{1}{\beta D} \tag{40}$$

and

$$\omega_{\mathrm{B}} = \frac{1}{\sqrt{m}} \left[- \left(\frac{\partial^2 U_{\mathrm{eff}}}{\partial f^2} \right)_T \right]^{1/2} |\nabla_r f|_T \tag{41}$$

is the frequency of the unstable mode of the saddle. One can actually show that the same value would also be obtained by performing a normal mode analysis of the molecule at the saddle point. However, we have to use the potential with the metric correction (this becomes essential in dissociation–recombination reactions since there is no well defined saddle). Some applications of this formula will be discussed in Sections IV C and IV D.

We have presented a general theory of diffusion controlled reactions. The rate constant can be evaluated asymptotically for the case of a single saddle point which gives the general result eqn. (31). The quantities needed are the diffusion coefficients and the potential energy. The resulting expression can be related to the transition state rate constant. Note that our approach treats the molecule as fully flexible. If one considers rigid bond molecules the results will be different.[37] Our approach could be extended to the treatment of pseudorotating transition states such as is encountered in cyclohexane.[27]

IV Simulations and the intermediate regime

A Interpolation formula

In previous sections we evaluated rate constants in different limits. In reality one is interested in rate constants at a given collision rate or fiction and not in its limiting behavior. Fortunately, simple Padè-like interpolation formulae are able to predict the rate constants with reasonable accuracy as long as the assumptions in the limiting theories are met. The idea used in the following is that any process discussed so far can act as a rate limiting step. For a large class of models of isomerization reactions or recombination–dissociation reactions the overall rate constant k is then well approximated by

$$k^{-1} \approx k_{\mathrm{low}}^{-1} + k_{\mathrm{TST}}^{-1} + k_{\mathrm{diff}}^{-1} \tag{42}$$

where k_{low} is the low pressure energy activation rate constant and k_{diff} is the diffusion controlled rate constant. This can be thought of as a sum of characteristic times associated with each process. One encounters analogous relations in the analysis of linear networks, *i.e.* the resistance of resistors in series is given by a similar relation.

Comparison of simulation data shows that this kind of connection formula is usually accurate to within 10–20%. If the assumptions used to derive the limiting theories are not met, we cannot expect the connection formula to work. For example, in the low collision or low friction regime for isomerization one finds that the assumption of rapid statistical energy equipartitioning is often not met, at least for most model potential energy surfaces which we have studied.[38,39] The high friction regime is reasonably safe unless friction is extremely anisotropic, the barrier is unphysically low or there are non-Markovian effects in which the bath is very slow.[40]

B Simulations

To address the validity of such interpolation formulae we have performed extensive simulations on several systems of increasing complexity. The simulation data were obtained by using the reactive flux method. The full reactive flux method has been reviewed elsewhere.[9] We have also employed a powerful modification of the reactive flux method called the 'absorbing boundary method' invented by Straub and Berne.[41,42]

For simplicity we focus only on the BGK model[19,8] and the Kramers model.[4] These two models can be treated using ideas already introduced in preceding sections. Both models reduce to spatial diffusion in the high collision rate or high friction regimes. In the low collision limit these two models behave very differently however. The BGK model is essentially in the strong collision limit whereas the Kramers model is in the weak collision limit at low friction.

C Butane

Let us now consider a model of a butane molecule originally studied in equilibrium by Rebertus *et. al.*[43] The dynamical properties of this model were considered in a molecular dynamics simulation by Rosenberg *et. al.*[44] A stochastic simulation has been performed by Montgomery *et al.*[45] where the solvent was modeled by the BGK model. Their data of the rate constant as a function of collision frequency are shown in Fig. 1. We now explain these simulation data in terms of the theories already discussed. Our analysis will be based on the assumption that the barrier energy is high compared with the thermal energy, an assumption which is not really met. In this case the barriers between the metastable wells are only 3 and 5 times the thermal energy, respectively. We have to keep this fact in mind when comparing theory with simulation.

The dividing surface used is $\phi - \phi_T$ with ϕ_T the position of the *trans–gauche* saddle where we locate the transition state. The mass is isotropic so that the transition state rate constant for the reaction from the *trans* to *gauche* state [*cf.* eqn. (6)] is

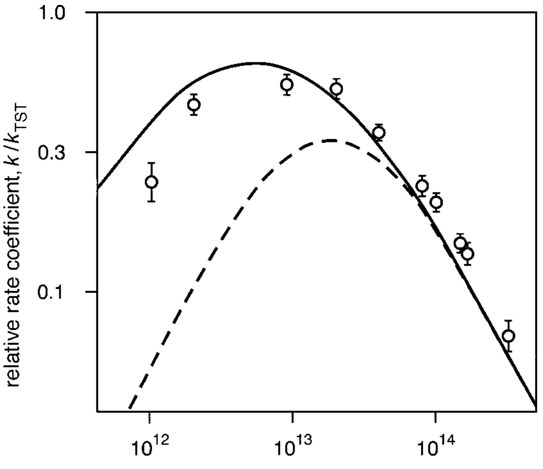

Fig. 1 Rate constant relative to the transition state result as a function of collision rate for the BGK model for butane. Solid line is the prediction of the Padè-like approximant eqn. (42) for the statistical theory for six degrees of freedom. The dashed line is the same theory applied to a single degree of freedom. Data points are simulation data with error bars obtained by Montgomery *et al.*[45]

$$k_{\mathrm{TST}} \approx \frac{|\nabla_{\boldsymbol{r}}\,\phi\,|_T}{\pi\sqrt{m}}\sqrt{\left(\frac{\partial^2 U}{\partial \phi^2}\right)_0}\,\mathrm{e}^{-\beta Q} \qquad (43)$$

where U is the dihedral angle potential. Note that this is actually twice eqn. (6) since we have two equivalent transition states for the reaction from the *trans* to *gauche* state. Furthermore, the Jacobian $[J(\boldsymbol{q}) = V 8\pi^2 r^2 s^2 t^2 \sin\theta_1 \sin\theta_2]$ for butane cancels exactly in eqn. (43) since it does not depend on the dihedral angle ϕ. Using the molecular dimensions given by Montgomery *et. al.*[45] we find that $|\nabla_{\boldsymbol{r}}\,\phi\,|_T \approx 1.5$ Å^{-1}. The dihedral potential is used to evaluate the second derivative and we obtain

$$k_{\mathrm{TST}} \approx 7.8 \times 10^{10}\ \mathrm{s}^{-1} \qquad (44)$$

which is in good agreement with $7.4 \times 10^{10}\ \mathrm{s}^{-1}$ reported by Montgomery *et. al.*[45] In the diffusion controlled regime we have

$$k_{\mathrm{diff}} = \frac{\omega_{\mathrm{B}}}{\alpha}\,k_{\mathrm{TST}} \qquad (45)$$

where

$$\omega_{\mathrm{B}} = \frac{|\nabla_{\boldsymbol{r}}\,\phi\,|_T}{\sqrt{m}}\sqrt{-\left(\frac{\partial^2 U}{\partial \phi^2}\right)_T} \approx 2.0 \times 10^{-13}\ \mathrm{s}^{-1} \qquad (46)$$

which is evaluated from the dihedral potential. The same value is found by performing normal mode analysis of the butane molecule in the transition state. In the low pressure regime the rate constant for activation from the *gauche* well ($\beta Q \approx 4.95$) is, in the strong collision approximation

$$k_{\mathrm{low}} \approx \alpha p\,\frac{(\beta Q)^5}{5!}\,\mathrm{e}^{-\beta Q} \approx 5.4 \times 10^{-2}\,\alpha \qquad (47)$$

where p is the trapping probability in the product (*gauche*) wells and where we used the low collision rate regime following from the multidimensional strong collision (SC) rate theory[46,47]

$$k_{\mathrm{SC}} = \alpha\,\frac{(\beta Q)^{n-1}}{(n-1)!}\,\mathrm{e}^{-\beta Q} \qquad (48)$$

Inserting eqn. (47) and the analogous expression for the reverse reaction into the detailed balance condition we find $p \approx 0.31$. This calculation used the harmonic approximation to evaluate the density of states and we have neglected the role of rotational degrees of freedom which could be treated using the approach already presented in the literature.[1,47] We insert these results into eqn. (42) and plot the resulting rate constant as a function of collision frequency in Fig. 1 (solid curve line). For comparison a one degree of freedom theory [using eqn. (43) instead eqn. (47)] is also shown (dashed line). Because of the extremely low barrier we have a quite atypical situation that the rate constant, in the low collision regime, is only one order of magnitude larger for six degrees of freedom than the corresponding rate constant for a single degree of freedom. In the case of a higher barrier the increase would be much more pronounced. One can see from Fig. 1 that the prediction of our theory is at worst within 50% of the simulation data. In the high collision regime the diffusive fall-off disagrees by 15% which is very good agreement keeping the low barrier height in mind. In the low collision regime the discrepancy is larger (50%). Keeping the fact in mind that the two wells in the problem are so shallow, such reasonable agreement is probably fortuitous. In light of this fact it is difficult to address the source of the discrepancies. In the high collision regime the discrepancy is almost certainly due to the asymptotic expansion used to derive eqn. (45). In the low collision regime the discrepancy can have several causes: harmonic approximation for the density of states, high barrier approximation, neglect of rotational contributions or non-RRKM effects. Nevertheless it is comforting to see that such a simple theory explains the simulation data in a reasonable fashion.

D Cyanide

As a last example we consider a triatomic molecule which can be thought to mimic HCN-isomerization. However, we do not attempt to model this reaction quantitatively. The potential, in reduced units, is given by

$$U = 700(1 - \mathrm{e}^{-2(s-0.9)})^2 + 400(1 - \mathrm{e}^{-2(r-0.57\cos^2\theta-0.78)})^2 + C\sin^2\theta \qquad (49)$$

where s is the CN distance, r is the distance from an H-atom to the midpoint of the CN bond and θ is the angle between these two distances. The two bonds are represented by deep Morse potentials and the angular coordinate moves over a $\sin^2\theta$ potential. A schematic contour plot of the potential as a function of the H-atom position for a fixed CN-bond length is shown in Fig. 2. The minima correspond to the two stable reactants (HCN and HNC). There are two saddle points corresponding to the transition states in which the molecule forms and equilateral triangle. The coupling of the modes comes only from the kinetic energy term. For simplicity we assume that all mass points have unit mass. We have performed simulations on this potential surface using the Kramers model where we assume that all the nuclei feel the same friction per unit mass. Some of the results are shown in Fig. 3. The theoretical predictions follow the same ideas as discussed previously. After some algebra the transition state theory gives [*cf.* eqn. (6)]

$$k_{\mathrm{TST}} \approx \frac{\omega_0}{3\pi}\,\mathrm{e}^{-\beta Q} \qquad (50)$$

where we have used

$$\omega_0 = \frac{2}{s_0}\sqrt{\frac{2C}{m}} \qquad (51)$$

Here $s_0 = 0.9$ and $m = 1$ in reduced units and we take $f = \cos\theta$. Since the Jacobian for a cyanide is,

$$J(\boldsymbol{q}) = V 8\pi^2 r^2 s^2 \sin\theta \qquad (52)$$

the ratio of the Jacobians $J(\boldsymbol{q}_T) : J(\boldsymbol{q}_0) = 1 : 3$. It is plausible that the centrifugal distortion makes the stable linear configu-

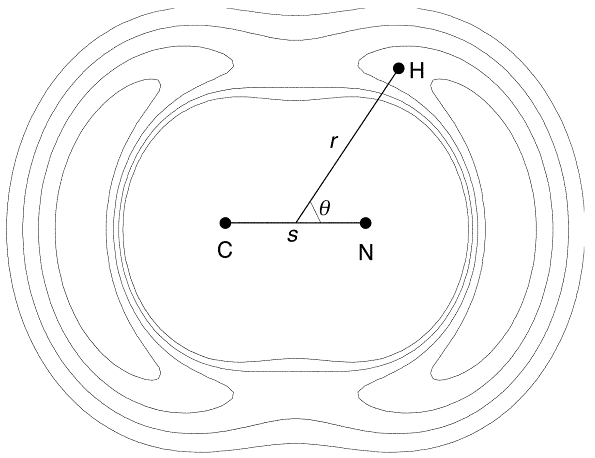

Fig. 2 Potential surface for the model HCN isomerization. We plot the potential energy for the position of the H-atom for fixed positions of the C and N-atoms.

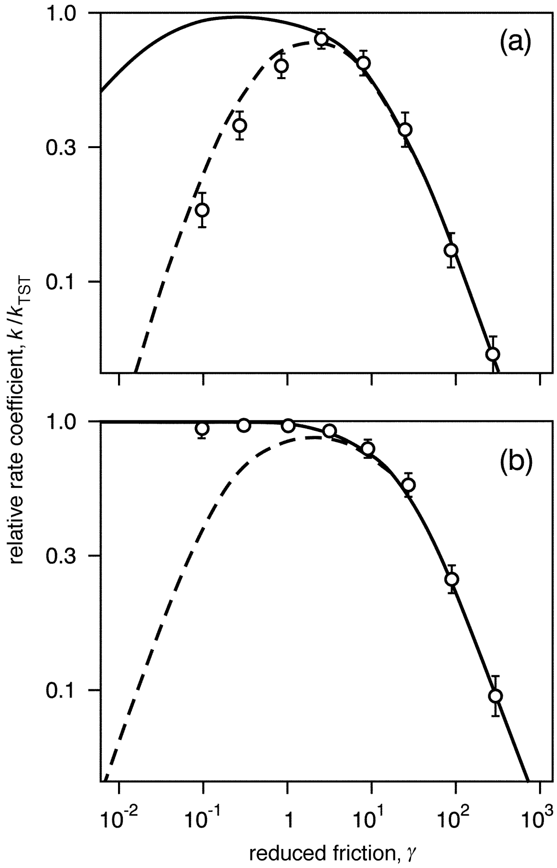

Fig. 3 Rate constants relative to the transition state result as a function of the friction for the Kramers model in the model HCN potential surface eqn. (49) with (a) $C = 25$ and (b) $C = 100$. Solid line is the prediction of the Padè-like approximant, eqn. (42), using a statistical three degrees of freedom theory. The dashed line is the same theory applied to a single degree of freedom. Data points are simulation data with 95% confidence intervals.

ration $\boldsymbol{q}_O$ more probable than the triangular transition state configuration $\boldsymbol{q}_T$. Note that eqn. (50) is twice eqn. (6) since we have two equivalent saddle points. In the diffusion controlled regime, we find that

$$k_{\text{diff}} = \frac{\omega_B}{\gamma} k_{\text{TST}} \tag{53}$$

where the barrier frequency $\omega_B = \omega_0$ which was introduced in eqn. (51). In the low friction region we employ the harmonic approximation, thus

$$k_{\text{low}} \approx \frac{\gamma}{2} \frac{(\beta Q)^3}{2} e^{-\beta Q} \tag{54}$$

and neglect the rotational effects for simplicity. The results are plotted in Fig. 3 for two cases: $C = 25$ [Fig. 3(a)] which is a potential surface with low frequencies and a lower barrier ($\beta Q = 10$), and $C = 100$ [Fig. 3(b)] which corresponds to a potential surface with higher frequencies and a higher barrier ($\beta Q = 40$). Note the excellent agreement between theory and simulation in the high friction, diffusion controlled regime. In the low friction regime the data do not follow the statistical three degrees of freedom theory at all. Rather, for the low barrier [low frequency surface ($C = 25$)] they follow the dashed line which is the one degree of freedom theory [$k_{\text{low}} \approx (\gamma/2)\beta Q \exp(-\beta Q)$] instead of eqn. (54). For the high barrier [high frequency surface ($C = 100$)] the simulation data seem to lie in between the one and three degree of freedom theories. Unfortunately, it is computationally too expensive to extend the simulations to lower frictions. All this means that the kinetic energy coupling is not effective enough to assure rapid energy partitioning on the energy shell. In this model we have severe non-RRKM effects which reduce the rate constant compared to the prediction of a statistical theory at low frictions.

References

1 P. Hanggi, P. Talkner and M. Borkovec, *Rev. Mod. Phys.*, 1990, **62**, 251.
2 B. J. Berne, M. Borkovec and J. E. Straub, *J. Phys. Chem.*, 1988, **92**, 3711.
3 C. W. Gardiner, *Handbook of Stochastic Methods*, Springer, New York, 1983.
4 H. A. Kramers, *Physica*, 1940, **7**, 284.
5 T. Yamamoto, *J. Chem. Phys.*, 1960, **33**, 281.
6 J. C. Keck, *Discuss. Faraday Soc.*, 1962, **33**, 173.
7 D. Chandler, *J. Chem. Phys.*, 1978, **68**, 2959.
8 J. A. Montgomery Jr., D. Chandler and B. J. Berne, *J. Chem. Phys.*, 1979, **70**, 4056.
9 B. J. Berne, in *Multiple Time Scales*, ed. J. U. Brackbill and B. I. Cohen, Academic Press, New York, 1985.
10 B. J. Matkowsky and Z. Schuss, *SIAM J. Appl. Math.*, 1977, **33**, 365.
11 W. L. Hase, *Dynamics of Molecular Collisions, Part B.*, ed. W. H. Miller, Plenum Press, New York, 1976.
12 J. Troe, *J. Chem. Phys.*, 1977, **66**, 4745.
13 W. Forst, *Theory of Unimolecular Reactions*, Academic Press, New York, 1982.
14 M. Smoluchowski, *Z. Phys. Chem.*, 1918, **92**, 129.
15 D. F. Calef and J. M. Deutch, *Annu. Rev. Phys. Chem.*, 1983, **34**, 493.
16 J. L. Skinner and P. G. Wolynes, *J. Chem. Phys.*, 1978, **69**, 2143.
17 J. L. Skinner and P. G. Wolynes, *J. Chem. Phys.*, 1980, **72**, 4913.
18 B. J. Berne, J. L. Skinner, and P. G. Wolynes, *J. Chem. Phys.*, 1980, **73**, 4314.
19 P. L. Bhatnagar, E. P. Gross and R. M. Krook, *Phys. Rev.*, 1954, **94**, 511.
20 R. F. Grote and J. T. Hynes, *J. Chem. Phys.*, 1980, **73**, 2715.
21 P. Pechukas, in *Dynamics of Molecular Collisions, Part B*, ed. W. H. Miller, Plenum Press, New York, 1976.
22 P. Pechukas, *Annu. Rev. Phys. Chem.*, 1978, **29**, 59.
23 D. G. Truhlar and B. C. Garrett, *Annu. Rev. Phys. Chem.*, 1984, **35**, 158.
24 E. B. Wilson, J. C. Decius and P. C. Cross, *Molecular Vibrations*, Dover, New York, 1980.
25 P. M. Rodger and M. G. Sceats, *J. Chem. Phys.*, 1985, **83**, 3358.
26 D. Chandler, in *Studies in Statistical Mechanics*, ed. E. W. Montroll and J. L. Lebowitz, North-Holland, Amsterdam, 1982.
27 H. M. Pickett and H. L. Strauss, *J. Am. Chem. Soc.*, 1970, **92**, 7281.
28 Z. Schuss and B. J. Matkowsky, *SIAM J. Appl. Math.*, 1979, **35**, 604.
29 B. J. Matkowsky, Z. Schuss and C. Tier, *J. Stat. Phys.*, 1984, **35**, 443.
30 J. S. Langer, *Ann. Phys. (NY)*, 1969, **54**, 258.
31 R. Landauer and J. W. Swanson, *Phys. Rev.*, 1961, **121**, 1668.
32 R. F. Grote and J. T. Hynes, *J. Chem. Phys.*, 1981, **74**, 4465.
33 G. van der Zwan and J. T. Hynes, *J. Chem. Phys.*, 1982, **77**, 1295.
34 P. Debye, *Trans. Electrochem. Soc.*, 1942, **82**, 265.
35 D. C. Torney and H. M. McConnel, *J. Phys. Chem.*, 1983, **87**, 1941.
36 J. Keizer, *J. Phys. Chem.*, 1981, **85**, 940.
37 D. C. Knauss and G. T. Evans, *J. Chem. Phys.*, 1980, **72**, 1499.
38 M. Borkovec, J. E. Straub and B. J. Berne, *J. Chem. Phys.*, 1986, **85**, 146.
39 J. E. Straub and B. J. Berne, *J. Chem. Phys.*, 1986, **85**, 2999.
40 J. E. Straub, M. Borkovec and B. J. Berneg, *J. Chem. Phys.*, 1985, **83**, 3172.
41 J. E. Straub and B. J. Berne, *J. Chem. Phys.*, 1985, **83**, 1138; J. E. Straub, D. A. Hsu and B. J. Berne, *J. Phys. Chem.*, 1985, **89**, 5188.
42 J. E. Straub, D. A. Hsu and B. J. Berne, *J. Phys. Chem.*, 1985, **89**, 5188.
43 D. W. Rebertus, B. J. Berne and D. Chandler, *J. Chem. Phys.*, 1979, **70**, 3395.
44 R. O. Rosenberg, B. J. Berne and D. Chandler, *Chem. Phys. Lett.*, 1980, **75**, 162.
45 J. A. Montgomery Jr., S. L. Holmgren and D. Chandler, *J. Chem. Phys.*, 1980, **73**, 3866.
46 M. Borkovec and B. J. Berne, *J. Chem. Phys.*, 1985, **82**, 794.
47 B. J. Berne, M. Borkovec and J. E. Straub, *J. Phys. Chem.*, 1988, **92**, 3711.

Paper 8/05781H